Broadband spectral measurements of diffuse optical properties by an integrating sphere instrument at the National Institute of Standards and Technology

Paul Lemaillet*, [a], Jeeseong Hwang[b], Heidrun Wabnitz[c], Dirk Grosenick[c], Lin Yang[c], and David W. Allen[a]

[a]National Institute of Standards and Technology, 100 Bureau Drive, Gaithersburg, MD 20899, USA

[b]National Institute of Standards and Technology, 325 Broadway Street, Boulder, CO 80305, USA

[c]Physikalisch-Technische Bundesanstalt (PTB), Abbestrasse 2-12, 10587 Berlin, Germany

ABSTRACT

Diffuse materials that approximate the optical properties of human tissue are commonly used as phantoms. In order to use the phantoms in a manner that provides consistent results relative to independent measurements, the optical properties need to be tied to a physics-based scale. Such a scale is needed for volume scattering of diffuse materials and this is currently being addressed by the development of a sphere based optical scattering reference instrument at the National Institute of Standards and Technology (NIST). Previous work towards that goal was constrained to the use of several laser lines at discrete wavelengths. Current work has expanded the spectral range for contiguous coverage. Here we report measurement results of the optical properties of solid phantoms, using two different base materials, acquired using NISTs diffuse optical properties reference instrument with visible or near infrared broadband illumination. The measurements of diffuse hemispherical reflectance and transmittance are analyzed using a custom inversion algorithm of the adding-doubling routine, and the expanded uncertainties on the results are provided. The broadband diffuse optical properties measured with the improved system agree to within the estimated uncertainty of the discrete measurements from two other institutes using alternative methods. This work expands the capabilities of the facility and can provide services for a wider range of applications.

Keywords: solid biomedical phantoms, integrating sphere, adding doubling, uncertainty budget, absorption coefficient, scattering coefficient, turbidity, broadband illumination.

1. INTRODUCTION

Biological phantoms are made of a mixture of scattering and absorbing materials in a liquid or in solid matrix and are used to mimic the optical properties of tissues in the development, characterization and maintenance of biomedical optical instruments. Scales for reflectance and transmittance are maintained by the National Institute of Standards and Technology (NIST). Such a scale is needed for volume scattering of diffuse materials and this need is currently being addressed by the development of an integrating sphere optical scattering reference instrument at NIST. The basic system and methods have been described in previous papers[1,2] and this paper presents the recent upgrade of the system to allow for broadband measurements of the absorption coefficient μ_a and the reduced scattering coefficient μ_s' in the visible range. Measurements of the optical properties of two types of solid biomedical phantoms are reported. The results are compared to measurements using time-domain measurement techniques.

*paul.lemaillet@nist.gov

Design and Quality for Biomedical Technologies X, edited by Ramesh Raghavachari, Rongguang Liang, Proc. of SPIE Vol. 10056, 1005604 · © 2017 SPIE · CCC code: 1605-7422/17/$18 · doi: 10.1117/12.2263338

2. MATERIAL AND METHODS

Two types of solid samples were measured. A polyurethane-based sample was provided by the Institut National d'Optique (INO, Quebec, Canada). The base material was mixed with titanium dioxide (TiO_2) powder to adjust μ_s' and with carbon black to adjust μ_a. The lateral dimensions of the INO sample were 100 mm square with a nominal thickness d=7 mm (measured thickness d=7.11 mm; uncertainty on d = 0.01 mm). The surface aspect of the sample slab was non-specular due to machining by INO. The nominal optical properties were μ_a=0.01 mm^{-1} and μ_s'=1 mm^{-1} at λ=800 nm (Fig. 1a).

Three polydimethylsiloxane (PDMS) samples with different concentration of added TiO_2 (2, 1 and 0.5 g/kg) were built at NIST. The samples were molded using plastic Petri dishes. Their diameter was 87 mm and their nominal thickness was d = 5 mm (measured thickness d = 4.85 mm for TiO_2 = 0.2 %, d = 4.29 mm for TiO_2 = 0.1 %, d = 4.32 mm for TiO_2=0.05 %; k = 1 uncertainty on d = 0.01 mm). The samples faces were specular (Fig. 1b).

(a) (b)

Figure 1: INO samples (a) and PDMS samples (b).

2.1 Integrating Sphere Optical Scattering Instrument

Figure 2 shows the experimental setup for the measurement of the optical properties of the samples. Two types of illumination are possible: one using a laser line from one of three options (HeNe laser: λ=543 nm, λ=632 nm;laser diode: λ=785 nm) and the other using a laser driven light source (LDLS, EQ 1500, Energetiq Technology Inc., MA, USA; broadband from 170 nm to 2100 nm). When down, a folding mirror FM allows the laser beam to reach the sample S. When FM is up, the broadband illumination of the sample is allowed.

The chosen laser beam (others being blocked by manual light shutter LS_1, LS_2 or LS_3) is directed toward the sample by a set of mirrors (M_1, M_2, M_3) and dichroic mirrors (DM_1, DM_2). The polarization of the laser beam is controlled by a polarizer P in front of a beam splitter BS_1. A portion of the beam power is detected by a photo-diode D_1 while the remaining portion of the beam power is normal-incident to the front face of the sample set at the sample port of an integrating sphere. The sphere is rotated 180° to measure the transmittance of the sample. The signal of the corresponding diffuse reflectance or total transmittance of the sample are detected by the photo-diodes D_2. Two current-voltage amplifiers (CV_1, CV_2) convert the photo-currents to voltages acquired by a data acquisition board (DAQ).

Broadband illumination from the LDSL is collimated by C_1 (biconvex lens, focal length f=30 mm) and the beam is converged to the tip of a fiber OF_1 by a parabolic mirror PM. At the output of the fiber, the beam is collimated by C_2 (biconvex lens, focal length f=25 mm) and directed by FM to a beam splitter BS_2 that divert a portion of the beam to the tip of a fiber OF_2 followed by a spectrometer SM_1 for reference purposes. Again, the remaining part of the beam is normal incident to the front face of the sample, the reflectance (transmittance) signal is detected by a fiber OF_3 followed by a spectrometer SM_2. The detection range of the spectrometer is 350 nm to 1050 nm.

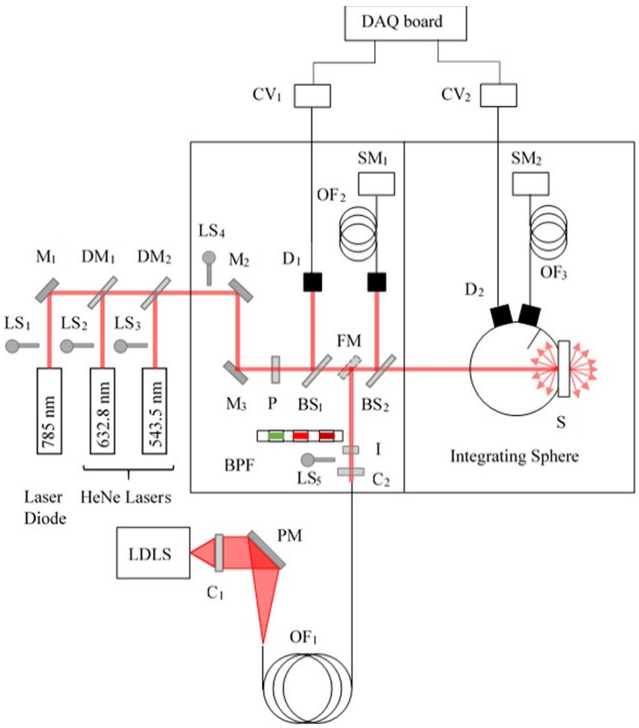

Figure 2: Schematic layout of the integrating sphere instrument; LDLS: laser-driven light source; LS_1, LS_2, LS_3, LS_4 and LS_5: light shutters; M_1, M_2 and M_3: mirrors; DM_1 and DM_2: dichroic mirrors; P, Glan-Taylor linear polarizer; BS_1 and BS_2: beam splitters; FM: folding mirror; C_1 and C_2: collimators; I: iris; D_1 and D_2: photodiodes; CV_1 and CV_2: current-voltage amplifiers; DAQ: data acquisition board; OF1, OF_2 and OF_3: optical fibers; SM_1 and SM_2: spectrometers.

2.2 Measurements and data analysis

The measurements are based on the substitution procedure which requires to compare the reflectance of the sample to the reflectance of a standard (NIST traceable standard R_{Std}=99 %) and the transmittance of the sample to the transmittance of a standard (100 % transmittance standard, *i.e.*, no sample). The measured reflectance is expressed as

$$R_{\text{Meas}} = R_{\text{Std}} \frac{I_{\text{Sample}}}{I_{\text{Standard}}} \tag{1}$$

where I_i are the normalized intensities computed as the ratio of the measured voltages from the signal and reference channels (i =Sample when the sample at the sample port of the spheres, i =Standard when R_{Std} is at the sample port of the reflectance sphere). Similarly, the measured transmittance is

$$T_{\text{Meas}} = \frac{I_{\text{Sample}}}{I_{\text{Empty}}} \tag{2}$$

where I_i are the normalized intensities computed as the ratio of the measured voltages from the signal and reference channels (i =Sample when the sample at the sample port of the spheres, i =Empty when no sample is present and the sample port of both spheres are in contact). All signals are corrected for a background signal obtained when a light shutter LS_4 (laser illumination) or LS_5 (broadband illumination) is closed. The details on how to make these measurements can be found elsewhere.[3,4]

The data analysis is based on the adding-doubling (AD) algorithm by Prahl[5] which solves the radiative transfer equation (RTE) using μ_a, the scattering coefficient μ_s , the thickness of the samples d, the anisotropy scattering parameter g and the index of refraction of the bulk material n as inputs. AD computes the total

reflectance and transmittance of a thin layer of material under the assumption of single scattering events (for which a solution of the RTE exits) and computes the total reflectance and transmittance of the sample by successively adding/doubling the values until the thickness of the sample is reached. The inversion procedure uses the measured voltages, the geometrical parameters of the spheres, d, n and g are input values to compute μ_a and $\mu_s' = (1-g)\mu_s$ as well as the total uncertainty budget. The inversion procedure was previously described in Ref.[1].

3. RESULTS

3.1 Polyurethane sample

Figure 3 presents the measurements of μ_a and μ_s' for $\lambda = 450\,\text{nm}$ to $850\,\text{nm}$. The values are compared to measurements made by INO at $\lambda = 475\,,\ 540\,,\ 543\,,\ 630\,,\ 632\,,\ 780\,,\ 805$ and $850\,\text{nm}$ using a time-domain transmittance measurement coupled to an analysis procedure based on Monte-Carlo simulations.[6] The uncertainty on the INO results were estimated using values from Ref.[6] that were computed for different samples at $\lambda = 600\,\text{nm}$. The results in Fig. 3a and 3b are presented with a coverage factor $k = 2$ ($2 \times \sigma$ error bars). There is a overlap in the results between NIST and INO over the wavelength range for both μ_a and μ_s' within the error bar at $k = 2$. Typical uncertainty values for the integrating sphere instrument are 5% on μ_a, 12% on μ_s' compared to 11% on μ_a, 7% on μ_s' for the INO results. Table 1 summarizes the results by INO and our results at $\lambda = [475\,,\ 540\,,\ 543\,,\ 630\,,\ 632\,,\ 780\,,\ 805\,,\ 850\,\text{nm}]$.

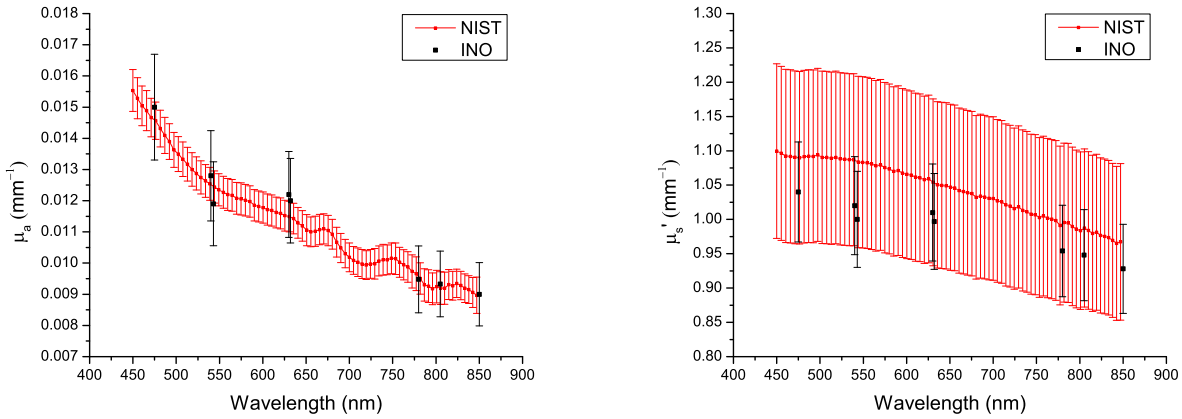

Figure 3: Broadband measurements of the absorption coefficient μ_a and the reduced scattering coefficient μ_s' for the INO sample using our single integrating sphere setup. The results are compared to the measurements by INO at $\lambda = 475\,,\ 540\,,\ 543\,,\ 630\,,\ 632\,,\ 780\,,\ 805$ and $850\,\text{nm}$.

3.2 PDMS samples

Figure 4 presents the measurements of μ_s' for $\lambda = 450\,\text{nm}$ to $850\,\text{nm}$ for PDMS samples with TiO_2 concentrations $0.05\,\%$, $0.1\,\%$ and $0.2\,\%$. The specular faces of the samples imply that for reflectance measurements at normal incidence, the specular reflectance is rejected through the entrance port of the integrating sphere. Hence, the measured reflectance is the diffuse reflectance and not the total reflectance expected by the adding-doubling algorithm. A correction for the Fresnel reflectance was introduced in a new version of our inversion algorithm to compensate for this. The values are compared to measurements made at the Physikalisch-Technische Bundesanstalt (PTB, Berlin, Germany) on thicker samples (about $12\,\text{mm}$ thick) from the same batch at $\lambda = 700\,,\ 750$ and $800\,\text{nm}$ using a time domain measurement technique.[7,8] In this case the optical properties were derived from measurements of time-resolved diffuse transmittance or reflectance that were conducted independently using two systems based on fast detectors and time-correlated single photon counting. One system used a Ti:Sapphire

Table 1: Results and uncertainties ($k = 2$) of: μ_a, the absorption coefficient of the sample; μ_s' the reduced scattering coefficient of the sample. The uncertainties on the INO results were estimated from measurements made on different samples at λ =600 nm as presented in Ref.[6].

λ (nm)	$\mu_a \times 10^{-3}$ (mm^{-1})		μ_s' (mm^{-1})	
	INO	NIST	INO	NIST
475	15.0 ± 1.7	14.60 ± 0.61	1.040 ± 0.073	1.09 ± 0.13
540	12.0 ± 1.6	12.50 ± 0.52	1.020 ± 0.071	1.09 ± 0.13
543	11.9 ± 1.3	12.50 ± 0.52	1.00 ± 0.07	1.08 ± 0.13
630	12.2 ± 1.4	11.50 ± 0.49	1.010 ± 0.071	1.05 ± 0.12
632	12.0 ± 1.4	11.50 ± 0.49	0.997 ± 0.070	1.05 ± 0.12
780	9.5 ± 1.1	9.49 ± 0.57	0.954 ± 0.067	0.99 ± 0.12
805	9.3 ± 1.1	9.23 ± 0.47	0.948 ± 0.066	0.98 ± 0.11
850	9.0 ± 1.0	8.92 ± 0.58	0.928 ± 0.065	0.97 ± 0.11

laser, free-space optics and a microchannel plate photomultiplier. The second system employed a supercontinuum laser with acousto-optic filter, optical fibers to guide the light to and from the sample and a hybrid photodetector. The time resolution of these systems was about 35 ps and 125 ps, respectively. The fit procedure for obtaining μ_s' and μ_a was based on the white Monte Carlo method, with a database of photon time-of-flight distributions created for multiple μ_s' values. The results presented here were obtained combining the data from both measurement systems.

The results in Fig. 4 are presented with a coverage factor $k = 2$. There is an overlap in the results between NIST and PTB. Typical uncertainty values on μ_s' for NIST are about 10% compared to 5% to 8% for PTB. Table 4 summarizes the results by PTB and our results at $\lambda = [700\,, 750\,, 800\,\text{nm}]$.

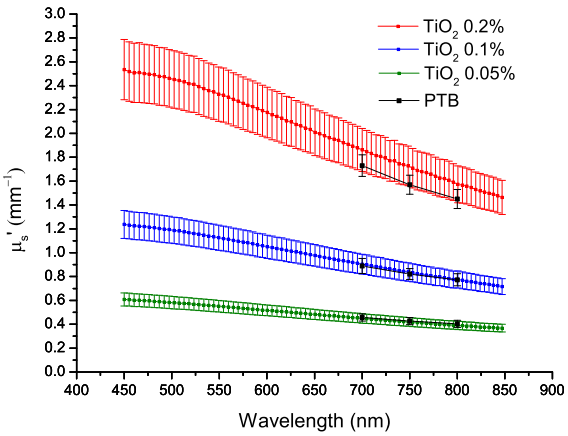

Figure 4: Broadband measurements of the reduced scattering coefficient μ_s' for the PDMS samples using the integrating sphere setup. The results are compared to the measurements by PTB at $\lambda = 700\,, 750$ and 800 nm.

4. CONCLUSION

In this paper we studied four solid samples, one non-specular polyurethane-based sample from INO and three specular PDMS-based samples built at NIST. The absorption coefficient μ_a of the INO sample and its reduced

Table 2: Results and uncertainties ($k = 2$) of the reduced scattering coefficient μ_s' of the PDMS samples as measured using the integrating sphere setup and the time domain measurement procedure used at PTB.

	λ (nm)	μ_s' (mm^{-1})	
		PTB	NIST
$TiO_2 = 0.05\%$			
	700	0.457 ± 0.030	0.449 ± 0.039
	750	0.427 ± 0.030	0.420 ± 0.037
	800	0.404 ± 0.030	0.391 ± 0.035
$TiO_2 = 0.1\%$			
	700	0.888 ± 0.063	0.904 ± 0.083
	750	0.821 ± 0.046	0.838 ± 0.077
	800	0.773 ± 0.051	0.776 ± 0.071
$TiO_2 = 0.2\%$			
	700	1.73 ± 0.09	1.86 ± 0.18
	750	1.57 ± 0.08	1.73 ± 0.17
	800	1.45 ± 0.08	1.57 ± 0.15

scattering coefficient μ_s' were measured using NIST's integrating sphere optical scattering instrument from $\lambda =$ 450 nm to 850 nm. The results were compared to the ones at $\lambda = 475\,, 540\,, 543\,, 630\,, 632\,, 780\,, 805$ and 850 nm provided by INO. There is an agreement between our results and the ones from INO within the error bar at $k = 2$. The uncertainty on our results were typically of 4% for μ_a and 12% for μ_s' compared to 11% and 7% respectively for INO. The reduced scattering coefficient μ_s' of the PDMS samples were measured at NIST for $\lambda =$ 450 nm to 850 nm. Typical uncertainty values at $k = 2$ on μ_s' for NIST were of 10% compared to 5% to 8% for PTB for measurements made at $\lambda =$ (700, 750 and 800) nm. There is an agreement between our results and the ones from PTB within the uncertainty range. Future work in developing this facility will include an inter-comparison study of PDMS samples between measurements using the integrating sphere instrument and goniometric measurements of the reflectance and the transmittance under normal illumination made using the the NIST spectral tri-function automated reference reflectometer (STARR) facility coupled with an analysis using a Monte Carlo-based model.[9,10]

ACKNOWLEDGMENTS

Certain commercial materials and equipment are identified in order to adequately specify the experimental procedure. Such identification does not imply recommendation by the National Institute of Standards and Technology. This work was supported by the NIST Innovation in Measurement Science (IMS) program. Authors thank Drs. Robert Hickernell and William Guthrie and Prof. Dr. Reiner Macdonald and Prof. Dr. Tobias Schffter for their support.

REFERENCES

[1] Lemaillet, P., Bouchard, J.-P., and Allen, D. W., "Development of traceable measurement of the diffuse optical properties of solid reference standards for biomedical optics at National Institute of Standards and Technology," *Applied optics* **54**(19), 6118–6127 (2015).

[2] Lemaillet, P., Bouchard, J.-P., Hwang, J., and Allen, D. W., "Double-integrating-sphere system at the National Institute of Standards and Technology in support of measurement standards for the determination of optical properties of tissue-mimicking phantoms," *Journal of biomedical optics* **20**(12), 121310–121310 (2015).

[3] Moffitt, T., Chen, Y.-C., and Prahl, S. A., "Preparation and characterization of polyurethane optical phantoms," *Journal of Biomedical Optics* **11**(4), 041103–041103 (2006).

[4] Lemaillet, P., Patrick, H. J., Germer, T. A., Hanssen, L., Johnson, B. C., and Georgiev, G. T., "Goniometric and hemispherical reflectance and transmittance measurements of fused silica diffusers," *SPIE Optical Engineering+ Applications* , 996109–996109, International Society for Optics and Photonics (2016).

[5] Prahl, S. A., van Gemert, M. J., and Welch, A. J., "Determining the optical properties of turbid media by using the adding–doubling method," *Applied optics* **32**(4), 559–568 (1993).

[6] Bouchard, J.-P., Veilleux, I., Jedidi, R., Noiseux, I., Fortin, M., and Mermut, O., "Reference optical phantoms for diffuse optical spectroscopy. part 1–error analysis of a time resolved transmittance characterization method," *Optics express* **18**(11), 11495–11507 (2010).

[7] Spinelli, L., Botwicz, M., Zolek, N., Kacprzak, M., Milej, D., Sawosz, P., Liebert, A., Weigel, U., Durduran, T., Foschum, F., et al., "Determination of reference values for optical properties of liquid phantoms based on intralipid and india ink," *Biomedical optics express* **5**(7), 2037–2053 (2014).

[8] Rothfischer, R., Grosenick, D., and Macdonald, R., "Time-resolved transmittance: a comparison of the diffusion model approach with monte carlo simulations," in [*European Conference on Biomedical Optics*], 95381H, Optical Society of America (2015).

[9] Lemaillet, P., Cooksey, C. C., Levine, Z. H., Pintar, A. L., Hwang, J., and Allen, D. W., "National Institute of Standards and Technology measurement service of the optical properties of biomedical phantoms: Current status," *SPIE BiOS* , 970002–970002, International Society for Optics and Photonics (2016).

[10] Levine, Z. H., Pintar, A. L., Cooksey, C. C., and Lemaillet, P., "Diffuse optical properties of a solid reference standard for biomedical optics," *Biomed. Express* (2017). Manuscript submitted for publication.